Influence of delaminations on fluid diffusion in multidirectional composite laminates – theory and experiments

Abedin I. Gagani*, Andreas T. Echtermeyer

Department of Mechanical and Industrial Engineering, Norwegian University of Science and Technology (NTNU), Trondheim, Norway

Abstract

Multidirectional composite laminates are often used in marine and offshore applications. Upon cyclic loading, cracks appear early in the off-axis plies and generate delaminations, which accelerate fluid diffusion. In this work, a theoretical model was developed for the prediction of fluid diffusion in laminates having cracks and delaminations. The model is based on the definition of a representative volume element subjected to Fickian diffusion. The geometry and dimensions of the representative volume element are determined by the crack density and the length of delaminations. Experiments were performed on both statically loaded samples having transverse cracks and fatigue loaded samples having transverse cracks and delaminations. The presence of delaminations increased the apparent diffusivity of the laminate by 5.4 times. The experimental results showed good agreement with the theory.

Keywords: Diffusion; Composite materials; Crack; Delamination; Environmental Degradation; Hygrothermal effect;

* Corresponding author.
E-mail address: abedin.gagani@ntnu.no (A. I. Gagani)

List of symbols

c	(-)	Moisture content
c_i	(-)	Length of i-th crack
C_i, D_j, E_k	(-)	1-D terms of 3-D solution of diffusion equation
c_{op}	(μm)	Crack opening
d	(mm)	Delamination length
d_{op}	(μm)	Delamination opening
D_{11}, D_{22}, D_{33}	(mm^2/h)	Composite orthotropic diffusion constants
D_{app}	(mm^2/h)	Composite apparent diffusion constant
D_{water}	(mm^2/h)	Water diffusion constant
h, h_0, h_{90}	(mm)	Laminate thickness, 0° ply thickness, 90° ply thickness
l	(mm)	Representative volume element length
L	(mm)	Sample length
m	(gr)	Mass of immersed samples
M	(%)	Moisture content %
$m_{composite}$	(gr)	Composite sample mass
$M_{eq}^{composite}$	(-)	Composite saturation moisture content
$M_{eq}^{cracked}$	(-)	Cracked composite saturation moisture content
m_i	(gr)	Initial mass
m_{water}	(gr)	Water mass
n	(-)	N° of plies in the laminate
$n_{90°}$	(-)	N° of 90° plies in the laminate
t	(hr)	Time
w	(mm)	Width
x, y, z	(-)	Cartesian coordinate system
$\rho_{composite}$	(gr/cm^3)	Composite density
ρ_{water}	(gr/cm^3)	Water density
ρ_w	(1/mm)	Crack density

1. Introduction

Composites materials used in marine and offshore environments are subjected to mechanical degradation in the form of stress rupture, fatigue and environmental degradation due to water or oil diffusion inside the material (Springer 1984, Weitsman and Elahi 2000).

Multidirectional laminates are typically used, as structures often are subjected to multiaxial loadings. Upon mechanical loading, transverse matrix cracks appear in the less favourably oriented plies (where fibres are not aligned with the load direction) at loads much lower than the ultimate load of the laminate (Gagani and Echtermeyer 2018).

When fatigue loads are applied to composite multiaxial laminates, transverse matrix cracks initiate delaminations developing from the crack tips (Kashtalyan and Soutis 2000, Carraro, Maragoni et al. 2017). This mechanism has been discussed in (Kashtalyan and Soutis 2000, Carraro, Maragoni et al. 2017), and is briefly schematized for simple cross-plied laminates in **Fig 1**.

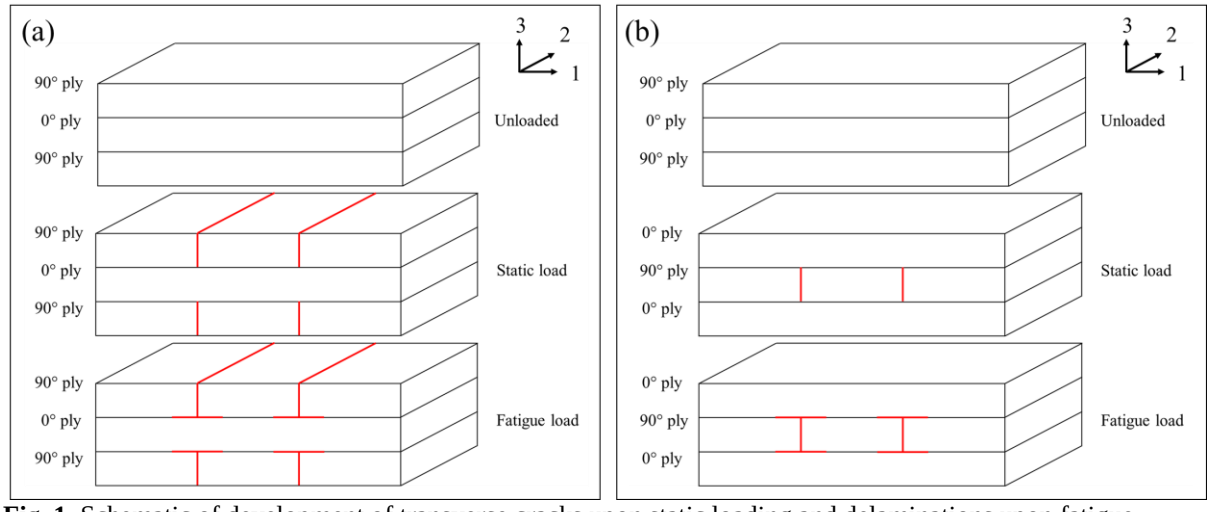

Fig. 1. Schematic of development of transverse cracks upon static loading and delaminations upon fatigue loading for (a) [90/0/90] and (b) [0/90/0] laminate

Several works have dealt with the effect of cracks on acceleration of fluid diffusion in composites, using both damage variable approaches (Weitsman 1987, Suri and Perreux 1995, Roy and Xu 2001, Roy, Xu et al. 2001) and continuum mechanics approaches

(Lundgren and Gudmundson 1998, Roy and Bandorawalla 1999, Gagani and Echtermeyer 2018).

Some works reported a small effect of cracks on fluid diffusivity of composites (Lundgren and Gudmundson 1999), while others reported greater effects (Suri and Perreux 1995, Roy and Bandorawalla 1999, Humeau, Davies et al. 2018). In (Gagani and Echtermeyer 2018) these results were compared, and it was noticed that cracks on the external layers - directly exposed to the fluid - accelerate greatly fluid diffusivity, while cracks on the internal layers did not. This effect was measured experimentally and analysed by a Fickian two-dimensional model where surface cracks and internal cracks were analysed separately. Furthermore, a finite element (FE) model was developed based on the work from (Roy and Bandorawalla 1999), giving the same results.

It can be intuitively envisioned that delamination can lead to even faster fluid ingress inside the material, hence faster saturation. However, to the best of the authors' knowledge there are no experimental results or theoretical models in the literature studying the effect of delaminations on fluid diffusion in composites.

In this work the theoretical model in (Gagani and Echtermeyer 2018), dealing with transverse matrix cracks, was extended to the case of laminates having transverse matrix cracks and delaminations. A Representative Volume Element (RVE) having cracks and delamination is defined. The solution proposed is analytical, based on series solution, but can be solved by means of FE analysis, as shown in (Gagani and Echtermeyer 2018) for the case of a laminate having transverse cracks.The model was compared to fluid diffusion experiments on fatigued samples that developed matrix cracks and delaminations. The model showed good agreement with experiments.

2. Material and methods

2.1. Materials

A glass fiber/epoxy composite laminate was manufactured using vacuum assisted resin transfer molding (VARTM). The matrix was Hexion Epikote™ Resin RIMR135 mixed with Epikure™ Curing Agent MGS RIMH137 with a mixing ratio of 100:30 by weight. Fibres used were HiPer-tex 0˚ UD glass fibers from 3B. Curing was performed at room temperature for 24 h and post-curing in a ventilated oven at 80˚C for 16 h.

The fiber volume fraction of the laminate was obtained by matrix burnoff testing, in accordance with the procedure reported in ASTM Standard D3171 (ASTM 2015), resulting in 54.2 %. The density of the samples was 1.93 g/cm^3.

Eighteen [90/0/90] tensile samples, were cut using a water-cooled diamond saw to dimensions 170 x 30 mm. Samples' thickness was 2.7 mm.

The material's mechanical properties were characterized in previous studies (Perillo, Vedvik et al. 2015). The strain to failure of these laminates was 2.4 % for a 0˚ laminate and 0.4 % for a 90 ˚ laminate.

2.2. Mechanical loading

The mechanical tests were performed using an Instron model 1342 servo hydraulic tensile machine having a load cell capacity of 50 kN. Six static tests were run under displacement control, with a strain rate of 1 mm/min up to 150 MPa and then unloaded, in order to induce transverse matrix cracks in the samples, which have been shown to appear for this load in (Gagani and Echtermeyer 2018). The tension-tension fatigue tests were carried out in load control, with a R-ratio of 0.1, a frequency of 7 Hz, and a maximum stress of 150 MPa, equivalent to the one used for the static tests. The fatigue testing induced delaminations growing from the transverse matrix cracks. Firstly, two samples were tested until failure,

which occurred at 263 860 and 306 781 cycles respectively, in order to find the cycles to failure of the laminate for this load. Then, six samples were loaded for 100 000 cycles and six samples were tested for 200 000 cycles. The intention of stopping the test before complete failure, was to developed transverse matrix cracks and delaminations without reaching failure of the 0° ply. Four plates were not tested, in order to provide a reference for the virgin material diffusion constants.

Fig.2 reports the dimension of the tensile samples. From each tensile coupon, a 50 mm long sample was obtained for diffusion testing from the central part, far from the tabs. The samples for diffusion testing were cut using a circular water-cooled diamond saw. Microscope analysis was performed in order to measure crack density. It showed that delaminations occurred only in fatigued samples, confirming that diamond saw cutting didn’t induce any delaminations.

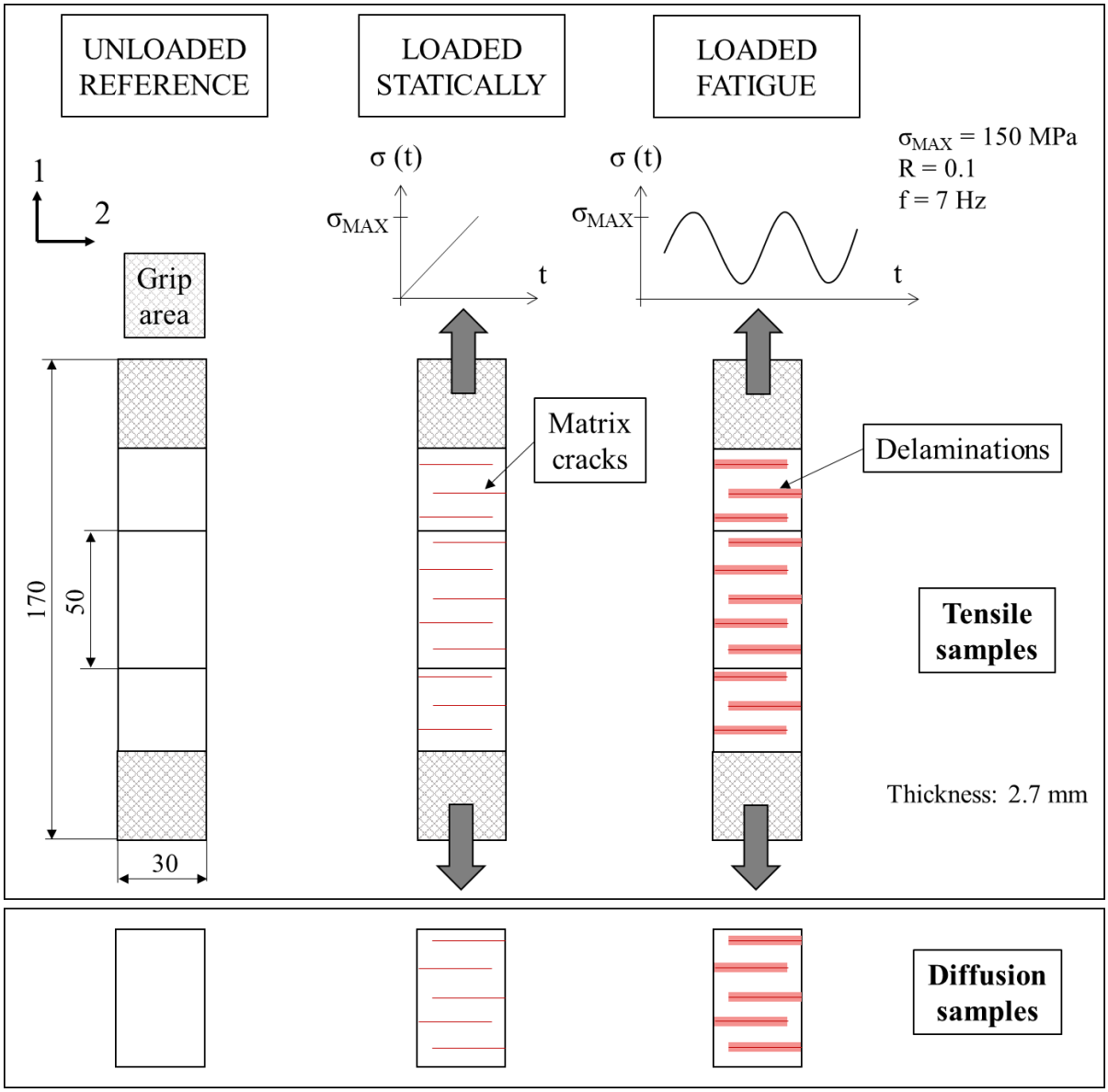

Fig. 2. Dimensions of the tensile coupons and of the diffusion sample.

Six repetitions were loaded for each loading case: static, 100 000 cycles fatigue and 200 000 cycles fatigue. For each case, four samples were conditioned in distilled water at 60°C and two samples were cut, ground, polished and analysed with an optical microscope in order to measure the crack parameters needed for the model: crack density, crack opening, delamination length and delamination opening. A summary of the samples tested is reported in **Table 1.**

Table 1
Overview of the samples tested

Configuration	No Load	Static load	100 000 cycles	200 000 cycles
Diffusion test	4 samples	4 samples	4 samples	4 samples
Microscope analysis	2 samples	2 samples	2 samples	2 samples

The samples used for the diffusion experiment are shown in **Fig. 3**. Cracks can be easily seen for the statically loaded samples and delaminations can be seen in addition for the fatigue loaded samples.

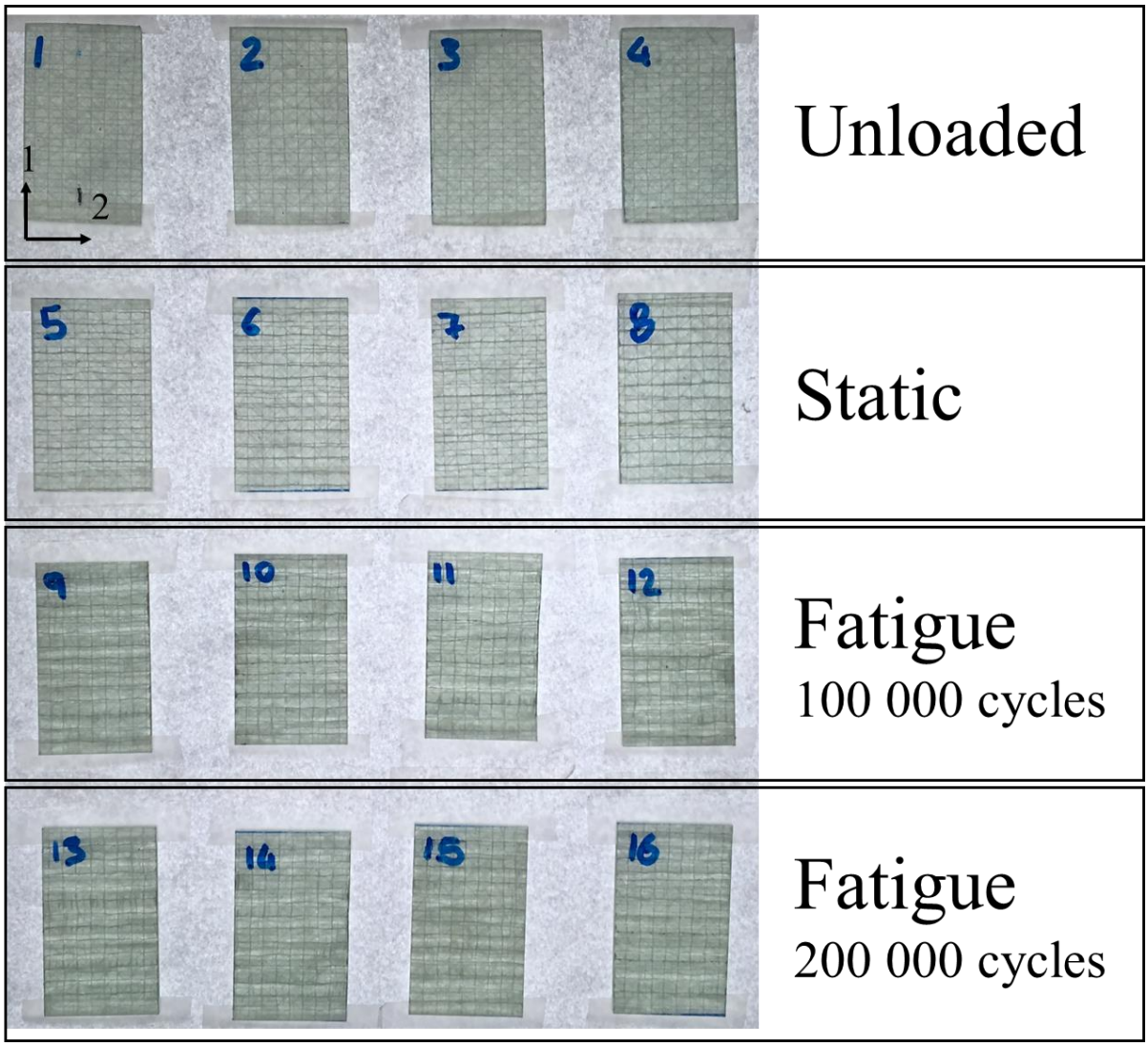

Fig.3. Samples before water conditioning.

2.3.Crack density measurements

For a cross-ply laminate, the weighted crack density is commonly defined as follows (Roy, Xu et al. 2001, Carraro, Maragoni et al. 2017):

$$\rho_w = \frac{\sum_{i=1}^{n°of\ cracks} c_i}{w\,L} \quad (1)$$

Where c_i is the length of each crack, w the width of the laminate and L is the length of the laminate.

The cracks' length c_i, was measured using a confocal microscope Alicona InfiniteFocus G4, counting the number of cracks present in the samples analysed. Crack densities obtained experimentally are reported in **Fig.4 (a)**. The average crack opening, c_{op}, defined as the distance between the opposite faces of the crack, is reported in **Fig. 4 (b)**.

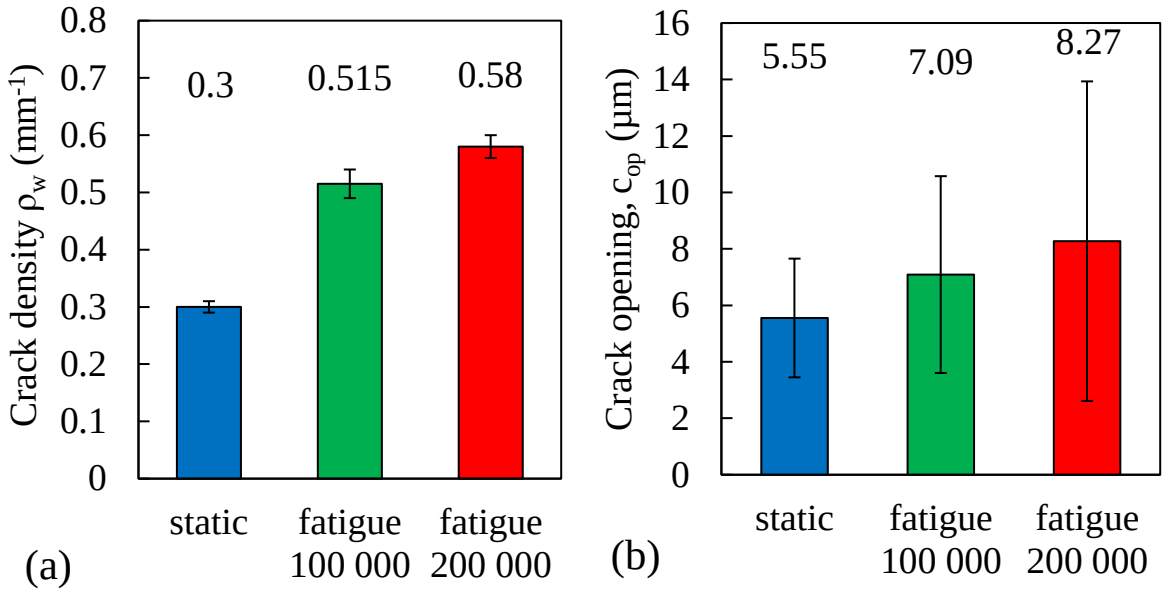

Fig. 4. (a) Crack density and (b) crack opening, for statically and fatigue loaded samples. Each result is based on the microscope analysis of two samples.

From the microscope analyses it was also possible to measure the average delamination length, **Fig. 5 (a)**, and the average delamination opening, **Fig. 5 (b)**, defined similarly to the crack opening. Since cracks and delaminations may have a non-uniform opening, the measurements were performed on several locations along the crack depth and along the delamination length, the results where the averaged. Local variations around the average would not influence the water uptake in any significant way.

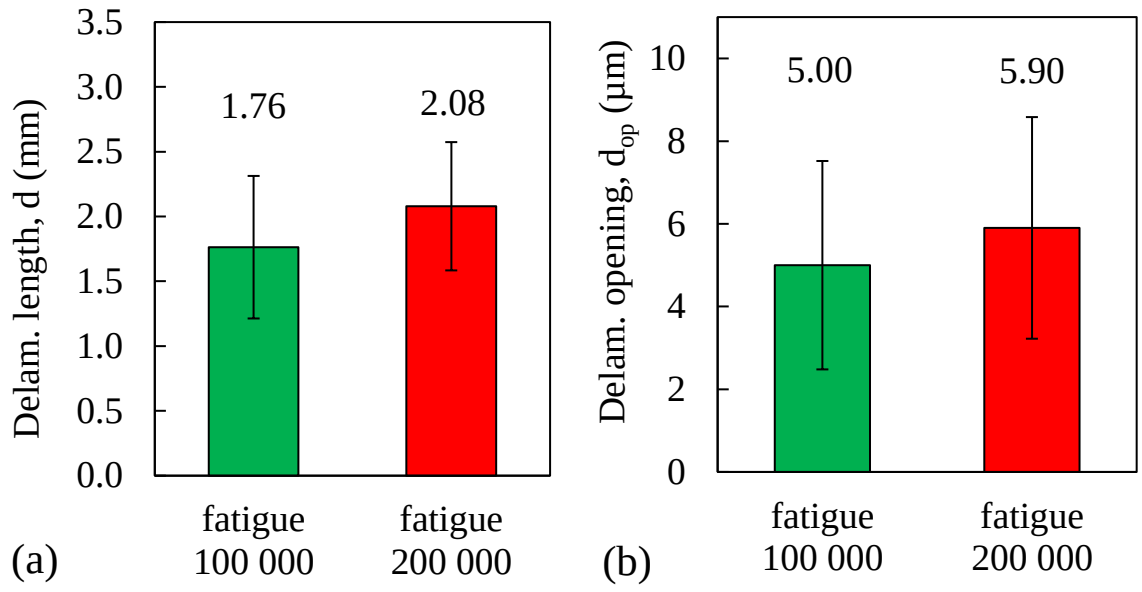

Fig. 5. (a) Average delamination length and (b) average delamination opening for fatigue loaded samples.

In **Fig. 6** an optical micrograph of a delamination starting from a transverse matrix crack in a fatigue loaded [90/0/90] laminate is shown. In a previous work of (Gagani and Echtermeyer 2018), it was noticed that cracks extended over the entire thickness of the 90° ply.

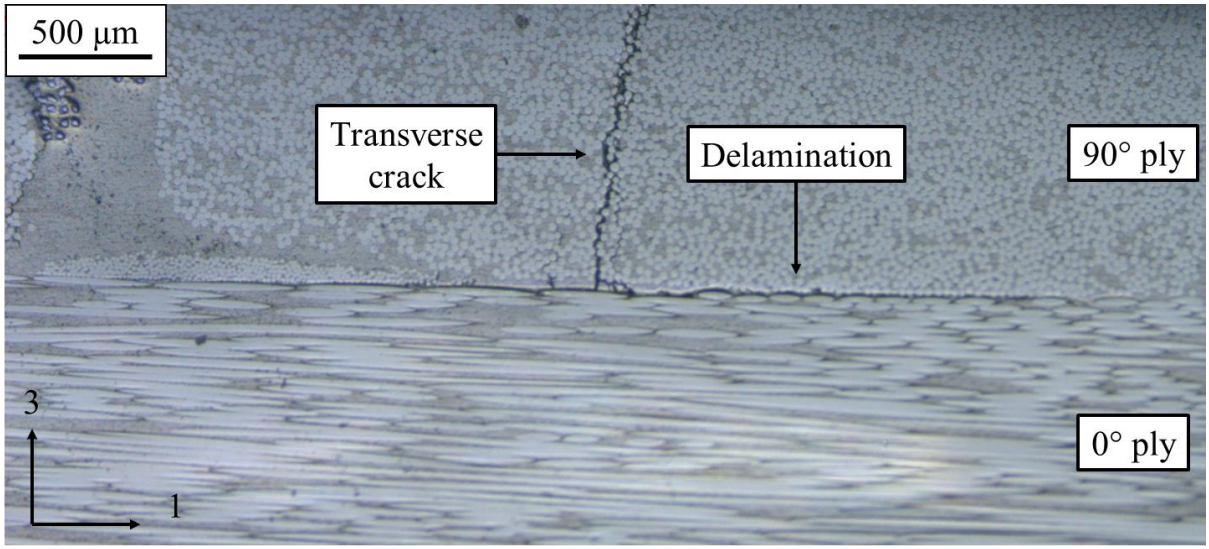

Fig. 6. Optical micrograph of crack and delamination in a fatigue loaded sample.

For glass fibre epoxy cross-plied laminates, the matrix cracks develop in the 90° plies already at 20% of ultimate strain.

The amount of water needed to fill a crack depends on the crack's size. It is important to take this aspect into account when modelling diffusion in cracked laminates. This is discussed in more detail in the model description.

2.4. Water uptake measurements

Samples were dried first for 144 hours in an oven at 40˚C, ensuring a stable and well defined starting point for the experiments (Gagani and Echtermeyer 2018). Conditioning in distilled water was subsequently done at 60˚C ± 1 ˚C. This temperature provides a convenient acceleration of the test without getting too close to the glass transition temperature of 84.7°C (HEXION 2006). Water was refilled regularly to provide always distilled and uncontaminated water. An aluminium holder was prepared and placed into the chamber to keep the samples in a vertical position and to avoid contact between them. This arrangement ensured that all faces of the samples were exposed to water.

In order to weigh the specimens, they were first taken out from the conditioning chamber and their surfaces were dried with a cloth. The weighing was done using a Mettler Toledo AG204 DeltaRange scale, having a sensibility of 0,1 mg and a capacity of 61 g. The samples weight was recorded and their moisture content was calculated following the ATSM standard for composite diffusion (ASTM 2014):

$$M(t) = 100 \cdot \frac{m(t) - m_i}{m_i} \tag{2}$$

where m_i was the initial dry mass, m(t) the recorded mass and M(t) the moisture content in %.

3. Analytical Model

An analytical model was developed here for predicting the moisture content of laminates having cracks and delaminations. For the sake of simplicity, the model presented here will

deal only with cross-plied laminates, containing only 0° and 90° plies, as the ones tested in this study. However, the approach can be extended to other laminate configurations.

The model is based on the following main assumptions and simplifications:

- Fick's equation is assumed to govern the diffusion problem;
- The transverse matrix cracks and delaminations are considered as empty volume, initially filled with air and able to host water proportionally to their volume;
- It is assumed that cracks and delaminations fill immediately with water. Capillary effects and water entrapment are not modelled. It was shown in (Roy and Bandorawalla 1999) that capillarity decelerates crack filling, but this process lasts in the range of seconds, while diffusion take typically several days.
- The transverse matrix cracks are assumed to be equally spaced. The presence of cracks and delaminations causes a change in the diffusion equation boundary conditions, as cracks and delaminations faces become exposed to water.
- The delaminations are assumed to start from each crack tip symmetrically. A delamination is assumed to be starting from each crack.
- The cracks and delaminations are assumed in this model to have a constant thickness and the delaminations are assumed to have a constant length along the width of the sample. This assumption is reasonable based on visual examination of the translucent samples. It should also be noted that average properties are governing water uptake, not local variations.

3.1. Moisture saturation content

The moisture saturation content of a laminate having transverse matrix cracks, can be estimated starting from the fundamental equation:

$$M_{eq}^{cracked} = M_{eq}^{composite} + \frac{m_{water}}{m_{composite}} \quad (3)$$

where $M_{eq}^{cracked}$ is the saturation moisture content of the cracked laminate, $M_{eq}^{composite}$ is the saturation moisture content of the virgin material, defined as the ratio between the mass of water absorbed at saturation by the undamaged material and the mass of the laminate. m_{water} is the mass of water trapped in the cracks and delaminations and $m_{composite}$ is the mass of the

laminate. From Eq. (3), it is possible to express the saturation moisture content $M_{eq}^{cracked}$ of the cracked laminate as follows:

$$M_{eq}^{cracked} = M_{eq}^{composite} + \frac{\rho_{water}\left(\frac{h}{n} c_{op} + d\, d_{op}\right) \sum_{i=1}^{n^{\circ} of\ cracks} c_i}{\rho_{composite}\, L\, w\, h} \tag{4}$$

Where h is the laminate thickness, n the number of plies, ρ_{water} is water´s density, $\rho_{composite}$ is composite´s density, c_{op} is the length of the crack opening, c_i is the length of the i-th crack, d the average length of the delaminations and d_{op} the average opening of the delaminations.

In Eq. (1), the total length of cracks was linked to the number of cracks. Expressing Eq. (1) in terms of crack density gives:

$$\frac{\sum_{i=1}^{p} c_i}{L\, w} = \rho_w \tag{5}$$

Substituting Eq. (5) in Eq. (4), the moisture saturation content of a laminate having transverse matrix cracks and delaminations can be predicted as:

$$M_{eq}^{cracked} = M_{eq}^{composite} + \frac{\rho_{water}\left(\frac{h}{n} c_{op} + d\, d_{op}\right) \rho_w}{\rho_{composite}\ h} \tag{6}$$

Eq. (6) predicts the moisture saturation content of a laminate having cracks and delaminations. It is important to correctly predict the moisture saturation content of the cracked laminate, because this value is needed to obtain the apparent diffusivity of the cracked and delaminated laminates, as will be shown in Eq. (24).

It is possible to notice that the expression for the moisture saturation content of a laminate having only transverse matrix cracks, without delaminations (Gagani and Echtermeyer 2018), is a particular case of Eq. (6), where the delamination term is null, $(d \cdot d_{op}) = 0$:

$$M_{eq}^{cracked} = M_{eq}^{composite} + \frac{\rho_{water}\, \rho_w\, c_{op}}{n\, \rho_{composite}} \tag{7}$$

3.2. Diffusivity prediction

Fick's second law for diffusion in orthotropic materials is (Crank 1956):

$$\frac{\partial c}{\partial t} = D_{11} \frac{\partial^2 c}{\partial x^2} + D_{22} \frac{\partial^2 c}{\partial y^2} + D_{33} \frac{\partial^2 c}{\partial z^2} \tag{8}$$

where c is the water concentration, *t* is time, *x*, *y* and *z* space coordinates and D_{11}, D_{22} and D_{33} diffusion constants in directions 1,2 and 3 respectively.

For a rectangular plate, formed only by 0° UD plies, having length L, width w and thickness h, the solution of the three dimensional anisotropic diffusion equation can be obtained by the method of separation of variables (Crank 1956, Roy and Bandorawalla 1999):

$$M(t) = M_{eq}^{composite}\left[1 - \left(\frac{8}{\pi^2}\right)^3 \sum_{i=1}^{\infty}\sum_{j=1}^{\infty}\sum_{k=1}^{\infty} C_i D_j E_k\right] \tag{9}$$

where the terms C_i, D_j and E_k consider 1-D mass flow respectively in thickness direction, length direction and width direction.

$$C_i = \frac{1}{(2i-1)^2} e^{-(2i-1)^2\left(\frac{\pi}{h}\right)^2 D_{33} t} \tag{10}$$

$$D_j = \frac{1}{(2j-1)^2} e^{-(2j-1)^2\left(\frac{\pi}{L}\right)^2 D_{11} t} \tag{11}$$

$$E_k = \frac{1}{(2k-1)^2} e^{-(2k-1)^2\left(\frac{\pi}{w}\right)^2 D_{22} t} \tag{12}$$

For a cross-plied laminate having a total of n-plies and $n_{90°}$-90° plies, the term of Eq. (9) dealing with through the thickness diffusion, C_i, remains unchanged, Eq. (10). The terms dealing with diffusion through the length and through the width of the laminate, D_j and E_k respectively, are modified as follows:

$$D_j = \frac{1}{(2j-1)^2} e^{-(2j-1)^2\left(\frac{\pi}{L}\right)^2 \frac{\left((n-n_{90°})D_{11}+n_{90°}D_{22}\right)}{n} t} \tag{13}$$

$$E_k = \frac{1}{(2k-1)^2} e^{-(2k-1)^2\left(\frac{\pi}{w}\right)^2 \frac{(n_{90°}D_{11}+(n-n_{90°})D_{22})}{n} t} \tag{14}$$

Eqs. (13,14) implicitly assume that for a cross-plied laminate, diffusion in length and width directions are a weighted average of the diffusivities of each ply. The validity of this assumption was assessed and confirmed in (Gagani and Echtermeyer 2018).

Substituting Eqs. (13,14) in Eq. (9), the expression for the weight gain of an un-cracked cross-ply laminate becomes:

$$M(t) = M_{eq}^{composite}\left[1 - \left(\frac{8}{\pi^2}\right)^3 \sum_{i=1}^{\infty}\sum_{j=1}^{\infty}\sum_{k=1}^{\infty} \frac{1}{(2i-1)^2} e^{-(2i-1)^2\left(\frac{\pi}{h}\right)^2 D_{33}t} \cdot \right.$$

$$\left. \frac{1}{(2j-1)^2} e^{-(2j-1)^2\left(\frac{\pi}{L}\right)^2 \frac{\left((n-n_{90^\circ})D_{11}+n_{90^\circ}D_{22}\right)}{n}t} \cdot \frac{1}{(2k-1)^2} e^{-(2k-1)^2\left(\frac{\pi}{w}\right)^2 \frac{(n_{90^\circ}D_{11}+(n-n_{90^\circ})D_{22})}{n}t}\right] \quad (15)$$

For a [90/0/90] laminate, having cracks in the external plies, as the ones statically loaded in this work, it is possible to model a representative volume element (RVE) having dimensions l, w and h. The terms w and h are the width and thickness of the laminate. The term l, RVE length, is a function of the crack density, as follows (Gagani and Echtermeyer 2018):

$$l = \frac{n_{90^\circ} L}{\rho_w L + 1} \quad (16)$$

The definition of the RVE is based on the geometry reported in **Fig. 7** and on the assumption of equally spaced cracks. About equally spaced matrix cracks are typically observed, e.g. experimental study by Mercier et al. (Mercier, Bunsell et al. 2008).

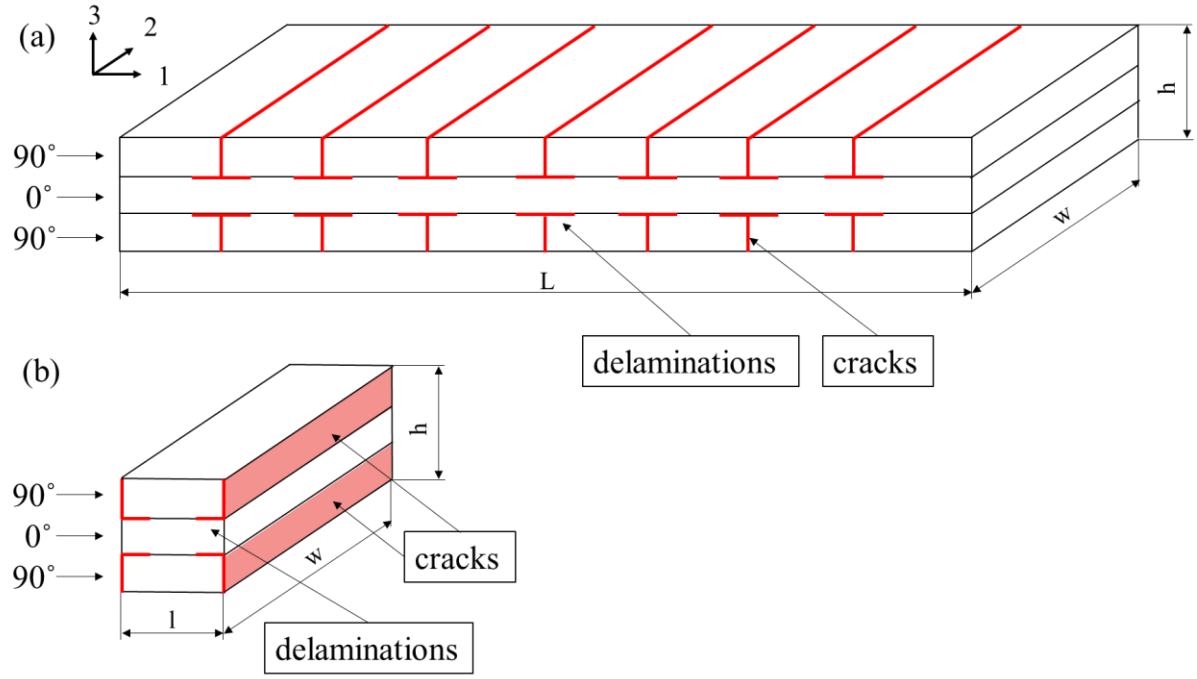

Fig.7. (a) Laminate and (b) RVE definition and dimensions.

It is assumed that cracks fill immediately with water, as discussed in (Gagani and Echtermeyer 2018), due to water diffusivity in air being ~ $10^6 \div 10^7$ times higher than in the composite, as suggested also by Lundgren and Gudmundson (Lundgren and Gudmundson 1999). Furthermore, in (Gagani and Echtermeyer 2018) it was shown that cracks on internal plies have a small effect on diffusivity, which can often be neglected, therefore in the current

study we will focus on laminates having cracks on the external plies. The cracks surfaces expose the faces of the RVE in **Fig. 7 (b)** to water. RVE dimensions are reported in **Table 2**.

The material´s orthotropic diffusion constants D_{11} and $D_{22} = D_{33}$, were obtained from a previous study on the same material (Gagani, Fan et al. 2018). The saturation moisture content was obtained from the weight gain measurements on un-cracked samples, since it is strongly dependent on the fibre volume fraction, (Gagani, Fan et al. 2018). The values are reported in **Table 3**.

Table 2
Values of RVE lengths, crack opening, delamination length and delamination opening

Configuration	l (mm)	c_{op} (µm)	d (mm)	d_{op} (µm)
Untested	50	-	-	-
Static	6.26	5.55	-	-
Fatigue 100 000 cycles	3.75	7.09	1.76	5.00
Fatigue 200 000 cycles	3.34	8.27	2.08	5.90

Table 3
Material properties used for the analytical model. The properties refer to 60° distilled water (Gagani, Fan et al. 2018).

Constituent	M_{eq} (-)	D_{11} (mm^2/h)	D_{22} (mm^2/h)	D_{33} (mm^2/h)
GF-Epoxy	0.82 %	0.02	0.0045	0.0045

The fluid diffusion of the RVE shown in **Fig. 8 (a)**, can be analysed as a parallel system made of five parallelepipeds subjected to water exposure, shown in **Fig 8 (b, c, d)**. Symmetry considerations allow isolating three type of parallelepipeds that describe the moisture absorption behaviour of the delaminated RVE: the central one, the two lateral ones and the four corner ones. Dimensions are shown in **Fig 8 (b, c, d)**.

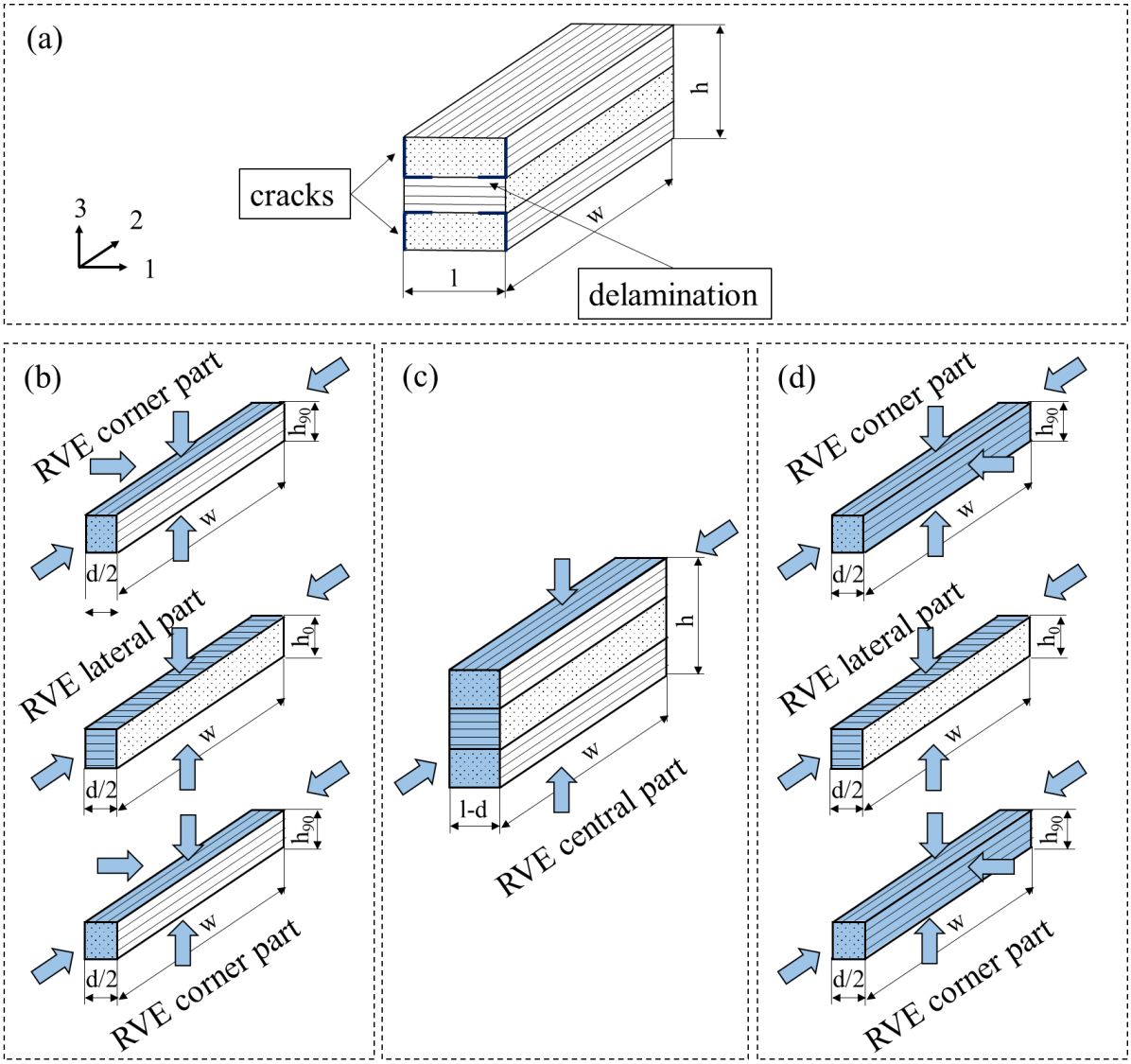

Fig.8. (a) RVE geometry and dimensions, (b) left lateral and corner parts of the RVE, (c) central part of the RVE, (d) right lateral and corner parts of the RVE. The colored surfaces of the RVE are exposed to water.

The moisture content of the central part of the RVE, **Fig. 8 (c)**, can be obtained by a two-dimensional diffusion solution, describing diffusion in the thickness and width direction:

$$M(t) = M_{eq}^{composite}\left[1 - \left(\frac{8}{\pi^2}\right)^2 \sum_{i=1}^{\infty}\sum_{j=1}^{\infty} \frac{e^{-(2i-1)^2\left(\frac{\pi}{h}\right)^2 D_{33} t}}{(2i-1)^2} \cdot \frac{e^{-(2j-1)^2\left(\frac{\pi}{w}\right)^2 \left(\frac{2\,D_{11}h_{90}+D_{22}h_0}{h}\right)t}}{(2j-1)^2}\right] \quad (17)$$

where h_0 is the thickness of the 0° ply and h_{90} is the thickness of the 90° ply.

For the lateral part of the RVE, shown in the middle in **Fig.8 (b), (d)**, the moisture content is obtained by another two-dimensional diffusion solution, describing diffusion in the thickness and width direction:

$$M(t) = M_{eq}^{composite}\left[1 - \left(\frac{8}{\pi^2}\right)^2 \sum_{i=1}^{\infty}\sum_{j=1}^{\infty} \frac{e^{-(2i-1)^2\left(\frac{\pi}{h_0}\right)^2 D_{33}t}}{(2i-1)^2} \cdot \frac{e^{-(2j-1)^2\left(\frac{\pi}{w}\right)^2 D_{22}t}}{(2j-1)^2}\right] \quad (18)$$

Finally, the moisture content of the corner parallelepiped of the RVE is obtained by a three-dimensional diffusion solution, describing diffusion in the thickness, width and length direction:

$$M(t) = M_{eq}^{composite}\left[1 - \left(\frac{8}{\pi^2}\right)^3 \sum_{i=1}^{\infty}\sum_{j=1}^{\infty}\sum_{k=1}^{\infty} \frac{e^{-(2i-1)^2\left(\frac{\pi}{h_{90}}\right)^2 D_{33}t}}{(2i-1)^2} \cdot \frac{e^{-(2j-1)^2\left(\frac{\pi}{d}\right)^2 D_{22}\,t}}{(2j-1)^2} \cdot \frac{e^{-(2k-1)^2\left(\frac{\pi}{w}\right)^2 D_{11}\,t}}{(2k-1)^2}\right] \quad (19)$$

It can be noticed that the term of Eq. (19) describing diffusion in the length direction takes into account the fact that only one of the faces of the parallelepiped is exposed to water in the length direction. For 1-D diffusion in a rectangle having only one exposed face, the length of the diffusion path needs to be multiplied by a factor two (Crank 1956), and the term *d* is used in Eq. (19) to describe diffusion from only one surface of the parallelepiped, having length *d/2*.

The final expression of the moisture content of a laminate having cracks and delaminations is obtained by summing the contributions of the three parallelepipeds in Eqs. (17) - (19):

$$M(t) = \frac{M_{eq}^{cracked}}{l\,h}\left[\left(1 - \left(\frac{8}{\pi^2}\right)^2 \sum_{i=1}^{\infty}\sum_{j=1}^{\infty} \frac{e^{-(2i-1)^2\left(\frac{\pi}{h}\right)^2 D_{33}t}}{(2i-1)^2} \frac{e^{-(2j-1)^2\left(\frac{\pi}{w}\right)^2\left(\frac{2\,D_{11}h_{90}+D_{22}h_0}{h}\right)t}}{(2j-1)^2}\right)\left(h\,(l - d)\right) + 2\left(1 - \left(\frac{8}{\pi^2}\right)^2 \sum_{i=1}^{\infty}\sum_{j=1}^{\infty} \frac{e^{-(2i-1)^2\left(\frac{\pi}{h_0}\right)^2 D_{33}t}}{(2i-1)^2} \frac{e^{-(2j-1)^2\left(\frac{\pi}{w}\right)^2 D_{22}t}}{(2j-1)^2}\right)\left(\frac{h\,d}{2}\right) + 4\left(1 - \left(\frac{8}{\pi^2}\right)^3 \sum_{i=1}^{\infty}\sum_{j=1}^{\infty}\sum_{k=1}^{\infty} \frac{e^{-(2i-1)^2\left(\frac{\pi}{h_{90}}\right)^2 D_{33}t}}{(2i-1)^2} \frac{e^{-(2j-1)^2\left(\frac{\pi}{d}\right)^2 D_{22}\,t}}{(2j-1)^2} \frac{e^{-(2k-1)^2\left(\frac{\pi}{w}\right)^2 D_{11}\,t}}{(2k-1)^2}\right)\right] \quad (20)$$

where $M_{eq}^{cracked}$ is computed according to Eq. (6). Substituting Eq. (6) in Eq. (20), the expression of the moisture content of a laminate having cracks and delaminations is:

$$M(t) = \frac{M_{eq}^{composite} + \frac{\rho_{water}\left(\frac{h}{n} c_{op} + d\, d_{op}\right)\rho_w}{\rho_{composite}\ h}}{l\, h} \left[\left(1 - \left(\frac{8}{\pi^2}\right)^2 \sum_{i=1}^{\infty}\sum_{j=1}^{\infty} \frac{e^{-(2i-1)^2\left(\frac{\pi}{h}\right)^2 D_{33} t}}{(2i-1)^2} \frac{e^{-(2j-1)^2\left(\frac{\pi}{w}\right)^2 \left(\frac{2\,D_{11}h_{90} + D_{22}h_0}{h}\right) t}}{(2j-1)^2}\right)\left(h\,(l-d)\right) + 2\left(1 - \left(\frac{8}{\pi^2}\right)^2 \sum_{i=1}^{\infty}\sum_{j=1}^{\infty} \frac{e^{-(2i-1)^2\left(\frac{\pi}{h_0}\right)^2 D_{33} t}}{(2i-1)^2} \frac{e^{-(2j-1)^2\left(\frac{\pi}{w}\right)^2 D_{22} t}}{(2j-1)^2}\right)\left(\frac{h\,d}{2}\right) + 4\left(1 - \left(\frac{8}{\pi^2}\right)^3 \sum_{i=1}^{\infty}\sum_{j=1}^{\infty}\sum_{k=1}^{\infty} \frac{e^{-(2i-1)^2\left(\frac{\pi}{h_{90}}\right)^2 D_{33} t}}{(2i-1)^2} \frac{e^{-(2j-1)^2\left(\frac{\pi}{d}\right)^2 D_{22}\, t}}{(2j-1)^2} \frac{e^{-(2k-1)^2\left(\frac{\pi}{w}\right)^2 D_{11}\, t}}{(2k-1)^2}\right)\right] \quad (21)$$

The moisture content of a laminate having cracks, but no delaminations was derived in (Gagani and Echtermeyer 2018), and is reported below:

$$M(t) = M_{eq}^{cracked} \left[1 - \left(\frac{8}{\pi^2}\right)^3 \sum_{i=1}^{\infty}\sum_{j=1}^{\infty}\sum_{k=1}^{\infty} \frac{e^{-(2i-1)^2\left(\frac{\pi}{h}\right)^2 D_{33} t}}{(2i-1)^2} \cdot \frac{e^{-(2j-1)^2 \frac{\left(\frac{\pi}{l}\right)^2 n_{90^\circ} D_{22}}{n} t}}{(2j-1)^2} \cdot \frac{e^{-(2k-1)^2\left(\frac{\pi}{w}\right)^2 \frac{\left(n_{90^\circ} D_{11} + \left(n - n_{90^\circ}\right) D_{22}\right)}{n} t}}{(2k-1)^2}\right] \quad (22)$$

where $M_{eq}^{cracked}$ was computed according to Eq. (5). Substituting Eq. (5) in Eq. (22), the expression of the weight gain of a laminate having cracks is:

$$M(t) = \left(M_{eq}^{composite} + \frac{\rho_{water}\, \rho_w\, c_{op}}{n\, \rho_{composite}}\right) \left[1 - \left(\frac{8}{\pi^2}\right)^3 \sum_{i=1}^{\infty}\sum_{j=1}^{\infty}\sum_{k=1}^{\infty} \frac{e^{-(2i-1)^2\left(\frac{\pi}{h}\right)^2 D_{33} t}}{(2i-1)^2} \cdot \frac{e^{-(2j-1)^2 \frac{\left(\frac{\pi}{l}\right)^2 n_{90^\circ} D_{22}}{n} t}}{(2j-1)^2} \cdot \frac{e^{-(2k-1)^2\left(\frac{\pi}{w}\right)^2 \frac{\left(n_{90^\circ} D_{11} + \left(n - n_{90^\circ}\right) D_{22}\right)}{n} t}}{(2k-1)^2}\right] \quad (23)$$

It is important to remark that this model doesn't need any calibration. All calculations use only the base material´s diffusivity and geometric parameters of cracks and delaminations. This model is based on 3-D orthotropic diffusion theory, the contribution of water flow through the edges of the sample is taken into account.

4. Results and discussion

The increase of moisture content with time is plotted for all samples in **Fig.9**. Four conditions are reported: the reference uncracked samples, the statically loaded samples, having transverse matrix cracks and the fatigue loaded samples, having transverse matrix cracks and delaminations. For the fatigues samples two conditions have been tested, samples loaded for 100 000 cycles and samples tested for 200 000 cycles.

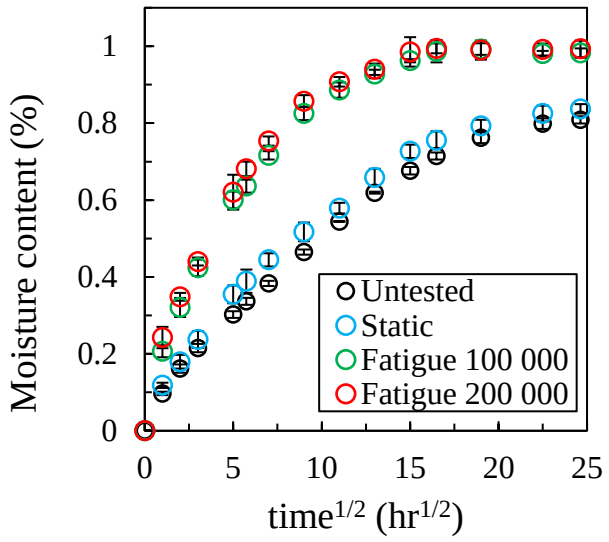

Fig. 9 Moisture content evolution for un-cracked, cracked and delaminated samples. Each point is the average of four replicates.

The acceleration of fluid diffusion in the cracked samples was quite limited, a trend consistent with the one reported in (Gagani and Echtermeyer 2018). For the samples subjected to cyclic fatigue loading, having transverse matrix cracks and delaminations, this effect was dramatically higher. Both moisture saturation content and diffusivity increased strongly. The samples loaded cyclically for 100000 and 200000 cycles showed similar results. This effect is attributed to the similar crack density, crack opening, delamination opening and delamination length of these samples, as shown in **Figs. 4-5**.

In **Fig. 10**, the experimental results were compared to the moisture content curves predicted analytically. The weight gain curve for the untested samples was predicted using Eq. (15), the

cracked weight gain curve using Eq. (23) and the delaminated weight gain curves using Eq. (21). The material properties used were reported in **Tables 2-3**.

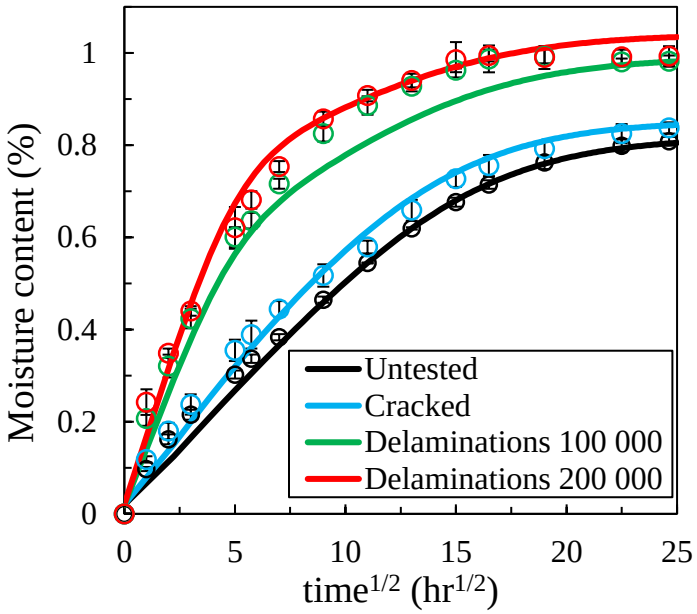

Fig. 10 Experimental and predicted moisture content evolution for un-cracked, cracked and delaminated samples

A quantitative comparison of the experimental results and predictions can be obtained by defining the apparent diffusivity of the laminates from the slope of the weight gain curves, according to 1-D Fickian diffusion theory (ASTM 2014):

$$D_{app} = \pi \left(\frac{h}{4M_{eq}}\right)^2 \left(\frac{\Delta M}{\Delta\sqrt{t}}\right)^2 \qquad (24)$$

The apparent diffusivity of the cracked laminate could be estimated by deriving Eq. (21), according to Eq. (24), however a simplified approach has been chosen here.

The slope of the moisture content curve was evaluated in the initial linear part, defined as the interval between 0 and 0.4% moisture content in **Fig. 10.** The results are summarized in **Table 4**.

The only parameter that was fitted in this model, was the moisture saturation content of the virgin material (no cracks or delaminations), as this parameter is strongly influenced by the fibre volume fraction and void content. The orthotropic diffusion constants of the virgin

(untested) material were obtained in a previous study of on the same material (Gagani, Fan et al. 2018). The theoretical calculations very accurately predict the experimental results. The prediction of the moisture saturation content for the cracked samples was also quite accurate. The predictions of both the moisture saturation content and apparent diffusivity were within the experimental standard deviation, **Table 4**. For the samples having delaminations, some predictions were less accurate, but still satisfactory. For the samples subjected to cyclic fatigue loading for 100000 cycles, the moisture saturation content prediction was very accurate, while the prediction of apparent diffusivity was less accurate, with a 21% deviation from the experimental results. For the samples subjected to cyclic fatigue loading for 200000 cycles, the predictions were very accurate. Both moisture saturation content and apparent diffusivity predictions were within a deviation of 4%. Overall the accuracy of the predictions was considered quite satisfactory.

Table 4
Experimental results and theoretical predictions of moisture saturation content and apparent diffusivity.

	Moisture saturation content (%)		*Apparent diffusivity (mm^2/h)*	
	Experimental	Analytical	Experimental	Analytical
Untested	0.82 ± 0.009	0.82	0.0057 ± 0.00016	0.0055
Static	0.84 ± 0.012	0.85	0.0067 ± 0.00064	0.0067
Fatigue 100 000 cycles	0.99 ± 0.029	0.99	0.029 ± 0.0030	0.023
Fatigue 200 000 cycles	1.00 ± 0.025	1.04	0.031 ± 0.0014	0.030

In **Fig.11**, the apparent diffusivity of statically and fatigue loaded samples is reported with respect to the base material diffusivity. It can be noticed that the samples loaded statically show a quite limited increase in apparent diffusivity, this effect is attributed to the limited influence of transverse matrix cracks on diffusivity. For the samples subjected to cyclic fatigue loading, the increase of apparent diffusivity is very drastic: 5.1 times for the samples

tested to 100000 cycles and 5.4 times for the samples tested to 200000 cycles. This effect is attributed to the presence of delaminations, which cause a strong increase of the surface exposed to fluid diffusion. From **Fig. 11**, it can be noticed that the analytical solutions reported in this work enable quite accurate predictions of fluid diffusivity for both statically and fatigue loaded samples, provided the matrix crack density and length of delaminations is known.

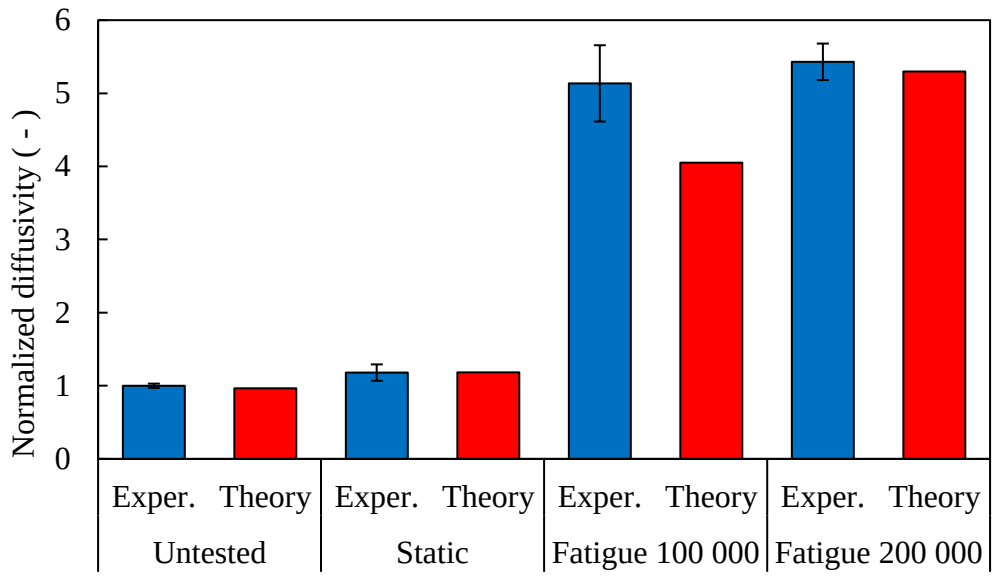

Fig.11. Experimental and theoretical predicted increase in apparent diffusivity. The values have been normalized with the respect to the untested material diffusivity: 0.0057 mm^2/h.

It is possible to analyse the scatters in the diffusivities of cracked and delaminated samples by considering the variations related to the optical microscopy experimental measurements of crack density, crack opening, delamination length and delamination opening.

For the diffusivity measured for the untested samples, a very small scatter was reported, 3 %, **Table 4** and **Fig.11**. The diffusivities of the cracked samples and delaminated samples showed higher scatters, between 5 and 11%. The higher scatters for the loaded samples are attributed to the scatters of crack density, crack opening, delamination opening and

delamination length, which were shown in **Figs. 4-5**. It should also be noted that the cracks were assumed to be equally spaced. This is not exactly true and may add to the scatter observed.

Considering the higher scatters reported for these measurements it may seem surprising to observe a limited scatter in the overall weight gain curves. The parameters that were measured for the development of the model were crack density, ρ_w, crack opening, c_{op}, delamination length, d, and delamination opening, d_{op}. The diffusivity of the delaminated samples was dependent on only two of these parameters, the crack density, ρ_w and the delamination length, d, which determined respectively the length of the RVE and of its sub-units, shown in **Fig. 8**. The crack density measurement showed a very limited scatter, **Fig. 4(a)** and the delamination length showed a higher but moderate scatter, **Fig 5(a)**. This is believed to be the reason for the quite limited experimental scatters on the diffusivity obtained from the weight gain measurements, **Fig. 9**.

Similarly, also the limited scatters reported for the measurements of the moisture saturation content of cracked and delaminated samples can be explained. Although the moisture saturation content is depended on all of four of the parameters measured by optical microscopy (crack density, crack opening, delamination length, delamination opening), it is more influenced by the parameters related to the length of damage created channels (crack density and delamination length) than on the parameters related to the width of such channels (crack opening and delamination opening).

For marine and offshore structures, where transverse matrix cracks appear during the operational life, it should be discussed whether only static loading are expected to occur during service life or fatigue loading too. In the first case, the influence of cracks on fluid diffusion, hence degradation can be negligible, especially for thicker laminates. Unfortunately, fatigue loading is often expected, due to periodical nature of environmental

loads, like waves. In this case, it is very likely that delaminations will grow from the tips of transverse matrix cracks. Delaminations associated with transverse matrix cracks have a strong influence on the acceleration of fluid diffusion and should therefore be accounted for.

Conclusions

A theoretical model was developed for the prediction of diffusivity in delaminated laminates, based on the definition of a representative volume element (RVE). The geometry and dimensions of the RVE are determined by the crack density and the length of delaminations. The model was compared to experiments on [90/0/90] laminates that were statically loaded before conditioning, to induce transverse matrix cracks and laminates subjected to cyclic fatigue loading, to induce additional delaminations.

The presence of cracks caused a slight increase in apparent diffusivity of 18% while the presence of delaminations caused a strong increase in apparent diffusivity, up to 540%. The model predicted both situations quite well.

Acknowledgements

This work is part of the DNV GL led Joint Industry Project “Affordable Composites” with nine industrial partners and the Norwegian University of Science and Technology (NTNU). The authors would like to express their thanks for the financial support by The Research Council of Norway (Project 245606/E30 in the Petromaks 2 programme).

Declarations of interest

None

References

ASTM (2014). Standard Test Method for Moisture Absorption Properties and Equilibrium Conditioning of Polymer Matrix Composite Materials, ASTM International, West Conshohocken, PA.

ASTM (2015). Standard Test Methods for Constituent Content of Composite Materials, ASTM International, West Conshohocken, PA.

Carraro, P. A., L. Maragoni and M. Quaresimin (2017). "Prediction of the crack density evolution in multidirectional laminates under fatigue loadings." Composites Science and Technology **145**: 24-39.

Crank, J. (1956). The mathematics of diffusion. Oxford, Clarendon Press.

Gagani, A., Y. Fan, A. H. Muliana and A. T. Echtermeyer (2018). "Micromechanical modeling of anisotropic water diffusion in glass fiber epoxy reinforced composites." Journal of Composite Materials **52**(17): 2321-2335.

Gagani, A. I. and A. T. Echtermeyer (2018). "Fluid diffusion in cracked composite laminates – Analytical, numerical and experimental study." Composites Science and Technology **160**: 86-96.

HEXION (2006). Technical Data Sheet. EPIKOTE Resin MGS RIMR 135 and EPIKURE Curing Agent MGS RIMH 137

Humeau, C., P. Davies and F. Jacquemin (2018). "An experimental study of water diffusion in carbon/epoxy composites under static tensile stress." Composites Part A: Applied Science and Manufacturing **107**: 94-104.

Kashtalyan, M. and C. Soutis (2000). "The effect of delaminations induced by transverse cracks and splits on stiffness properties of composite laminates." Composites Part A: Applied Science and Manufacturing **31**(2): 107-119.

Lundgren, J.-E. and P. Gudmundson (1998). "A Model for Moisture Absorption in Cross-Ply Composite Laminates with Matrix Cracks." Journal of Composite Materials **32**(24): 2226-2253.

Lundgren, J.-E. and P. Gudmundson (1999). "Moisture absorption in glass-fibre/epoxy laminates with transverse matrix cracks." Composites Science and Technology **59**(13): 1983-1991.

Mercier, J., A. Bunsell, P. Castaing and J. Renard (2008). "Characterisation and modelling of aging of composites." Composites Part A: Applied Science and Manufacturing **39**(2): 428-438.

Perillo, G., N. Vedvik and A. Echtermeyer (2015). "Damage development in stitch bonded GFRP composite plates under low velocity impact: Experimental and numerical results." Journal of Composite Materials **49**(5): 601-615.

Roy, S. and T. Bandorawalla (1999). "Modeling of Diffusion in a Micro-Cracked Composite Laminate Using Approximate Solutions." Journal of Composite Materials **33**(10): 872-905.

Roy, S. and W. Xu (2001). "Modeling of diffusion in the presence of damage in polymer matrix composites." International Journal of Solids and Structures **38**(1): 115-126.

Roy, S., W. Xu, S. Patel and S. Case (2001). "Modeling of moisture diffusion in the presence of bi-axial damage in polymer matrix composite laminates." International Journal of Solids and Structures **38**(42–43): 7627-7641.

Springer, G. (1984). Environmental Effects on Composite Materials, Technomic Publishing Company.

Suri, C. and D. Perreux (1995). "The effects of mechanical damage in a glass fibre/epoxy composite on the absorption rate." Composites Engineering **5**(4): 415-424.

Weitsman, Y. (1987). "Coupled damage and moisture-transport in fiber-reinforced, polymeric composites." International Journal of Solids and Structures **23**(7): 1003-1025.

Weitsman, Y. J. and M. Elahi (2000). "Effects of Fluids on the Deformation, Strength and Durability of Polymeric Composites – An Overview." Mechanics of Time-Dependent Materials **4**(2): 107-126.